RAA 2014 Vol. **14** No. **10**, 1307–1328 doi: 10.1088/1674–4527/14/10/010
http://www.raa-journal.org *http://www.iop.org/journals/raa*

Research in Astronomy and Astrophysics

Application of two special orbits in the orbit determination of lunar satellites *

Peng Liu[1,2], Xi-Yun Hou[1,2], Jing-Shi Tang[1,2] and Lin Liu[1,2]

[1] School of Astronomy and Space Science, Nanjing University, Nanjing 210093, China; *silence@nju.edu.cn*
[2] Institute of Space Environment and Astrodynamics, Nanjing University, Nanjing 210093, China

Received 2013 September 4; accepted 2014 April 19

Abstract Using inter-satellite range data, the combined autonomous orbit determination problem of a lunar satellite and a probe on some special orbits is studied in this paper. The problem is firstly studied in the circular restricted three-body problem, and then generalized to the real force model of the Earth-Moon system. Two kinds of special orbits are discussed: collinear libration point orbits and distant retrograde orbits. Studies show that the orbit determination accuracy in both cases can reach that of the observations. Some important properties of the system are carefully studied. These findings should be useful in the future engineering implementation of this conceptual study.

Key words: celestial mechanics — space vehicles — Moon — methods: numerical

1 INTRODUCTION

Currently, navigation and guidance of lunar satellites mainly rely on the support from ground stations (Liu et al. 2003). With more and more lunar and deep space missions being planned, similar to NASA's Mars Deep Space Network (Bell et al. 2000), the idea of building a lunar satellite constellation has been proposed (Carpenter et al. 2004; Hill et al. 2005a,b). Such a constellation has many advantages: it can provide continuous communications between the Earth and the far side of the Moon (Li et al. 2007); it can provide navigation for lunar satellites and deep space probes passing by the Moon (Wang & Huang 2009); it can be combined with the ground stations to form a so called space VLBI to observe deep space targets (Hirabayashi et al. 2000); it can map the lunar gravitational field globally, not just on the nearside, to unprecedented accuracy and resolution (Hoffman 2009), etc.

All these applications require precise lunar orbits. Due to the long distance between the Earth and the Moon, measurement data (and correspondingly, the orbit determination (OD) accuracy) of lunar satellites from Earth suffer from the problem of low accuracy (km levels) and possible shelter from the Moon. The highly accurate inter-satellite range data, which are already used between Earth's satellites, are a good choice to enhance the OD accuracy (Kato et al. 2008). However, a well-known problem of merely using this type of data is the overall rotation of the constellation (i.e. undermined orbital inclination, ascending node and perigee) (Liu & Liu 2000). The usual solution

* Supported by the National Natural Science Foundation of China.

to this problem is to add support from a ground station (Liu et al. 2000) or support from some other external references (Yim et al. 2004; Sheikh et al. 2006). Of all these studies, the idea of the combined autonomous orbit determination (CAOD) between a collinear libration point (CLP) probe and a lunar satellite (Hill et al. 2005a,b) seems pretty interesting to us.

CLPs are special equilibrium points associated with the restricted three-body problem (RTBP) (Szebehely 1967). In the late 1960s, Colombo and Farquhar firstly proposed the application of CLPs in the Earth-Moon system (Farquhar 1967). Till now, about ten probes (ISEE-3, SOHO, ACE, etc) have flown in the Sun-Earth CLPs (Farquhar et al. 2004), but only two missions (ARTEMIS and GRAIL) have flown in the Earth-Moon CLPs (Folta et al. 2012; Chung et al. 2010). There are many advantages to using the CLPs in the Earth-Moon system. For example, probes around the CLPs can provide a continuous link between Earth and the far side of the Moon. In addition, they are possible candidates for lunar space stations (Farquhar 1972). Different from lunar satellites, CLP probes are in the region where the gravitational force of the Earth and the Moon are comparable to each other. The introduction of CLPs provides an absolute reference orientation for a lunar satellite. Due to this fact, CAOD of both the lunar satellite and the CLP probe is possible. In this paper, we extend the idea in Hill et al. (2006); Hill & Born (2007) and do further research on the CAOD problem between CLP probes and a lunar satellite. Some useful information such as the nominal orbits of the CLP probes and the configurations of the system has been found.

The CLP probe is not the only choice for the CAOD of a lunar satellite. Theoretically speaking, any kind of orbit that can provide an absolute reference orientation for a lunar satellite can play the same role as the CLP probe. In our study, another kind of special orbit—a distant retrograde orbit (DRO) around the Moon is also studied. The research shows that DROs are competitive with CLP orbits, not only because the results from OD are comparable to each other, but also because the DROs usually have much better stability properties than CLP orbits.

This paper is organized as follows: In Section 2, a brief introduction is made about the circular restricted three-body problem (CRTBP) model and the two special kinds of orbits used in our work. Section 3 gives some details about the CAOD process. In Section 4, the CAOD problem of a lunar satellite and CLP probes is studied in the CRTBP model, with some numerical simulations. Section 5 describes the CAOD problem of a lunar satellite and the DRO probes is studied in the CRTBP model, also with some numerical simulations. Section 6 contains the results that are generalized to the real force model of the Earth-Moon system. Section 7 has some discussions and conclusions are made in Section 8.

2 CRTBP, HALO ORBIT AND DRO

2.1 The CRTBP Model

The RTBP describes the motion of a massless small body under the gravitations of two massive bodies. The two massive bodies are called primaries. When the two primaries are on circular orbits, this model is reduced to the CRTBP model. For the Earth-Moon system at hand, the Earth and Moon are the two primaries and the CLP probe is the small body. Usually, the small body's motion is described in a frame rotating with the two primaries. This frame is called the synodic frame (Szebehely 1967).

It is well known that there are five libration points in the CRTBP. Theoretically speaking, small bodies can remain static on these libration points in the synodic frame.

Figure 1 shows the locations of these five libration points in the barycentric synodic frame. Three of them (L_1, L_2, L_3) are called collinear libration points, and the other two (L_4, L_5) are called triangular libration points. In this study, only L_1 and L_2 are our focus because they are closer to the Moon. In the synodic frame, the following dimensionless parameters are used

$$[M] = m_1 + m_2\,, \quad [L] = \overline{P_1P_2} = a\,, \quad [T] = \sqrt{a^3/G[M]}\,. \tag{1}$$

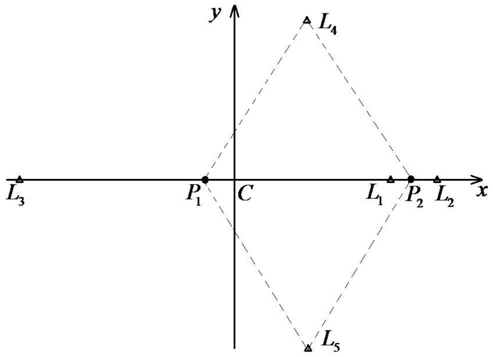

Fig. 1 The barycentric synodic frame and the five libration points.

The equation of motion of the probe is as follows

$$\ddot{\boldsymbol{r}} + 2(-\dot{y}, \dot{x}, 0)^{\mathrm{T}} = (\partial\Omega/\partial\boldsymbol{r})^{\mathrm{T}} , \tag{2}$$

where

$$\Omega = [x^2 + y^2 + \mu(1-\mu)]/2 + (1-\mu)/r_1 + \mu/r_2 \,. \tag{3}$$

Here $\mu = m_2/(m_1 + m_2)$; $m_1, m_2 (m_1 > m_2)$ are the masses of the two primaries and r_1, r_2 are the distances of the probe from the two primaries.

Usually, the motion of the lunar satellite is described in a Moon-centered inertial frame. However, the CLP orbits (or the DRO orbits) are described in the synodic frame. As a result, a transformation between the two frames is necessary. Denoting the state vectors in the barycentric synodic frame, the Moon-centered synodic frame and the Moon-centered inertial frame respectively as $(\boldsymbol{r}, \dot{\boldsymbol{r}})$, $(\boldsymbol{r}_1, \dot{\boldsymbol{r}}_1)$ and $(\boldsymbol{R}, \dot{\boldsymbol{R}})$, we have

$$\boldsymbol{r}_1 = \boldsymbol{r} - (1-\mu, 0, 0)^{\mathrm{T}}, \qquad \dot{\boldsymbol{r}}_1 = \dot{\boldsymbol{r}}, \tag{4}$$

$$\boldsymbol{R} = \boldsymbol{R}_z(-\theta)\boldsymbol{r}_1, \qquad \dot{\boldsymbol{R}} = \boldsymbol{R}_z(-\theta)\dot{\boldsymbol{r}}_1 + \dot{\boldsymbol{R}}_z(-\theta)\boldsymbol{r}_1, \tag{5}$$

where $\boldsymbol{R}_z(*)$ indicates the rotational matrix along the z axis, and θ is the rotation angle of the synodic frame with respect to the inertial frame (Szebehely 1967). $\mu = 0.0123000383$ is the mass parameter of the Earth-Moon CRTBP system.

2.2 Halo Orbits

Motions around the CLPs are generally unstable, but conditionally stable orbits can still exist, such as the well-known Lissajous orbits and halo orbits.

Figure 2 depicts one Lissajous orbit and one halo orbit around the L_1 point in the Earth-Moon system. Both kinds of orbits can be used as nominal orbits for the CLP probes. Halo orbits are usually preferable due to their periodicity and better visibility from Earth. In the following studies, we will focus on halo orbits. However, all the methods also apply for Lissajous orbits. Note that the length unit in Figure 2 and in the following figures (Figs. 3–7) is the mean distance between the Earth and Moon, i.e., 384747.981 km.

Using the third-order analytical solution (Richardson 1980) or even higher order analytical solutions (Jorba & Masdemont 1999) as the initial seed for the numerical correction algorithms that are applied to periodic orbits (Doedel et al. 2007), we can compute the halo orbits. In our work, a 15th

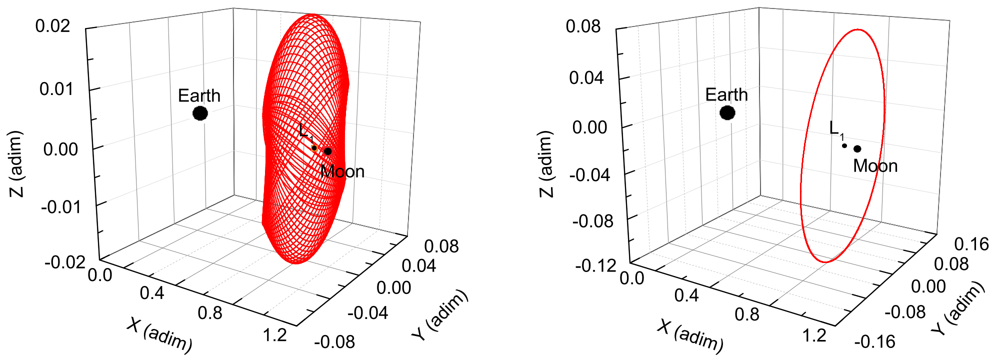

Fig. 2 Two kinds of conditionally stable orbits around the L_1 point in the Earth-Moon system. *Left*: Lissajous orbit; *Right*: halo orbit.

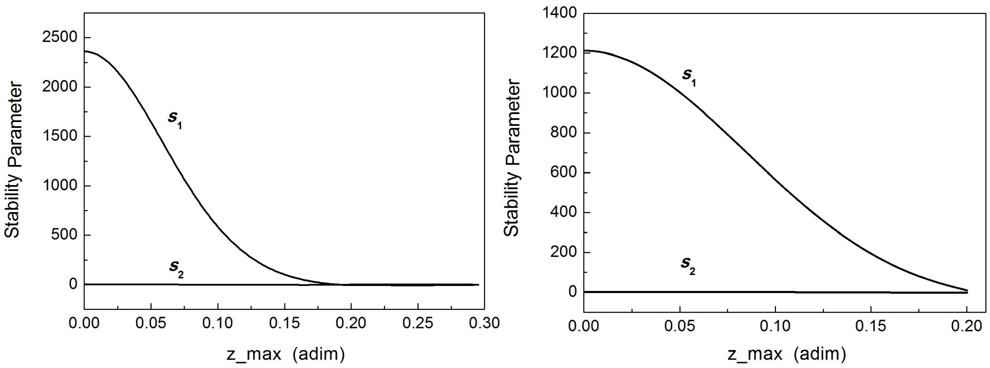

Fig. 3 The stability parameter versus the out-of-plane amplitude of the halo family around the point L_1 (*left*) and L_2 (*right*) in the Earth-Moon system.

order analytical solution is used as the initial seed and usually 2–3 iterations are enough to get the initial state of small halo orbits to the machine accuracy. Using the well-known predictor-corrector algorithm, we can go from smaller halo orbits to larger halo orbits (Muñoz-Almaraz et al. 2003). Due to nonlinear effects, some properties of the halo orbits such as period and stability also change with the orbital amplitude.

Denote the state vector of the small body as $\boldsymbol{X} = (\boldsymbol{x}, \boldsymbol{y}, \boldsymbol{z}, \dot{\boldsymbol{x}}, \dot{\boldsymbol{y}}, \dot{\boldsymbol{z}})$ and briefly denote Equation (2) as

$$\dot{\boldsymbol{X}} = \boldsymbol{F}(\boldsymbol{X})\,. \tag{6}$$

Starting from the initial point $\boldsymbol{X}_0 = \boldsymbol{X}(t_0 = 0)$, the trajectory under Equation (6) can be denoted as

$$\boldsymbol{X}(t) = \boldsymbol{X}(\boldsymbol{X}_0, t)\,. \tag{7}$$

A periodic orbit (such as the halo orbit) satisfies

$$\boldsymbol{X}(t = T) - \boldsymbol{X}_0 = 0\,, \tag{8}$$

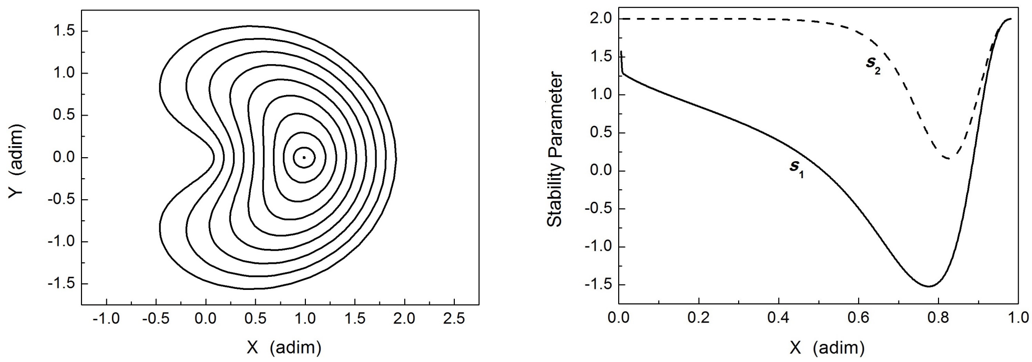

Fig. 4 Some examples of the DRO family (*left*) and the stability curves of this family (*right*).

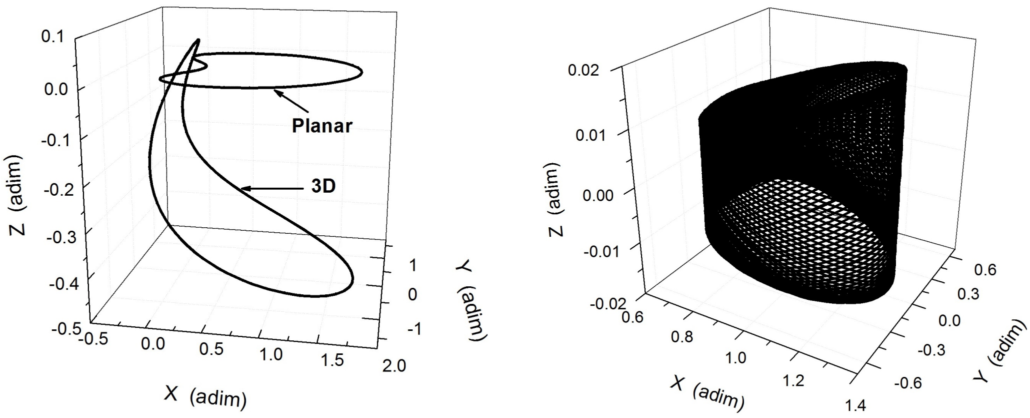

Fig. 5 *Left*: the vertical critical orbit in the DRO family and one member of the spatial family bifurcating from it. *Right*: a quasi-periodic orbit produced by adding a vertical displacement from a planar DRO.

where T is the period of the orbit. The monodromy matrix of a periodic orbit is defined as

$$\boldsymbol{M} = \frac{\partial \boldsymbol{X}(t)}{\partial \boldsymbol{X}_0}|_{t=T} \,, \tag{9}$$

where the right hand side of Equation (9) is the state transition matrix of the periodic orbit. For Hamiltonian systems such as the CRTBP, eigenvalues of the matrix $\boldsymbol{M}$ should appear in conjugate and in pairs (Arnol'd 1999). That is, if λ is an eigenvalue of $\boldsymbol{M}$, then $\bar{\lambda}, \lambda^{-1}, \bar{\lambda}^{-1}$ should also be eigenvalues of $\boldsymbol{M}$. For halo orbits with small to moderate amplitudes, the eigenvalues of $\boldsymbol{M}$ usually have the form (Gómez et al. 1998b)

$$(1, 1, a, a^{-1}, e^{ib}, e^{-ib}) \,, \tag{10}$$

where a, b are real numbers and usually $a \gg 1$ for halo orbits. Denoting the eigenvalue pair of the matrix $\boldsymbol{M}$ as $(\lambda_i, \lambda_i^{-1})$, the stability parameter is defined as Bray & Goudas (1967)

$$s_i = \lambda_i + \lambda_i^{-1} \,. \tag{11}$$

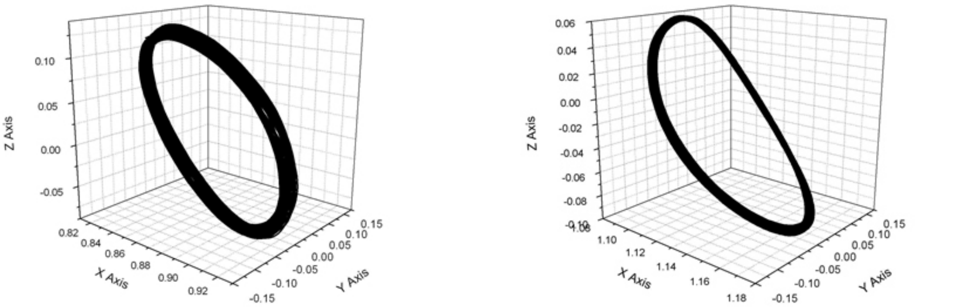

Fig. 6 One quasi-halo orbit around L_1 (*left*) or L_2 (*right*) in the real force model of the Earth-Moon system. The orbits last about two years, starting from the epoch J2000.0.

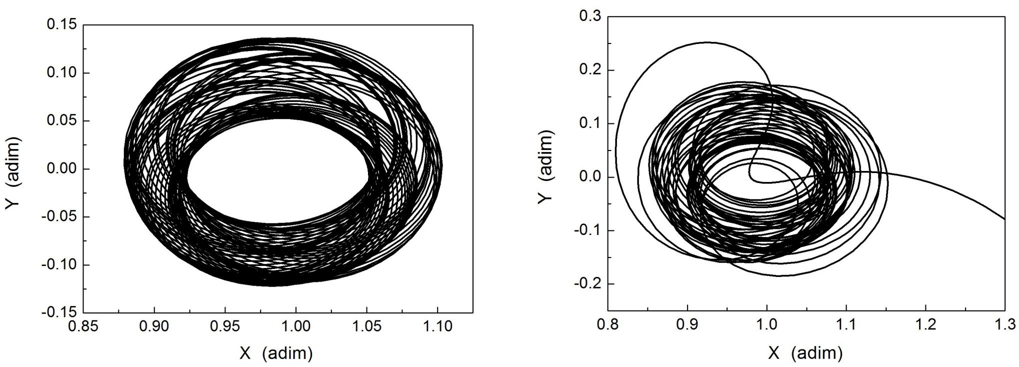

Fig. 7 Two DROs in the real force model. The left orbit has smaller amplitude and can remain in the proximity of the Moon even in the real force model. The right orbit has a larger amplitude and eventually escapes from the Moon after a number of orbits around it. The integration time is one year, starting from the epoch J2000.0. To save space, only projections on the $x - y$ plane are given.

Usually for the eigenvalue pair of $(\lambda_i, \lambda_i^{-1}) = (e^{ib}, e^{-ib}), b \neq 0, |s_i| < 2$, the motion is in the space spanned by the eigenvalues of this eigenvector pair and is linearly stable. For the eigenvalue pair of $(\lambda_i, \lambda_i^{-1}) = (a, a^{-1}), a \neq 1, |s_i| > 2$, the motion is linearly unstable. Generally, the parameter can be used as an indicator of the stability of the motion. The motion around the periodic orbit is stable if $|s_i| < 2$, unstable if $|s_i| > 2$ and critical if $|s_i| = 2$. For the more general case of $(\lambda_i, \lambda_i^{-1}) = (e^{c+ib}, e^{-c-ib})$, similar results apply. Due to nonlinear effects, the values of b, c will change and the case $b = c = 0$ may happen. In this case, we reach the critical point and a bifurcation may (not necessarily) occur (Doedel 1981). In fact, the family of halo orbits bifurcates from a vertical bifurcation member of the planar Lyapunov family around the collinear libration points (Hou & Liu 2013).

For a three dimensional periodic orbit in the CRTBP model, the eigenvalues of the monodromy matrix should satisfy (Bray & Goudas 1967)

$$(\lambda - 1)^2(\lambda^2 + p_1\lambda + 1)(\lambda^2 + p_2\lambda + 1) = 0, \tag{12}$$

where

$$\begin{aligned} p_1 &= \frac{1}{2}(\alpha + \sqrt{D})\,; \\ p_2 &= \frac{1}{2}(\alpha - \sqrt{D})\,; \\ D &= \alpha^2 - 4(\beta - 2)\,; \\ \alpha &= 2 - Tr(M)\,; \\ \beta &= \frac{1}{2}[\alpha^2 + 2 - Tr(M^2)]. \end{aligned} \tag{13}$$

Obviously $s_i = -p_i$.

Due to the following symmetry of Equation (2)

$$(x, y, z, \dot{x}, \dot{y}, \dot{z}, t) \quad \longleftrightarrow \quad (x, y, -z, \dot{x}, \dot{y}, -\dot{z}, t). \tag{14}$$

Actually we have two families of halo orbits around each CLP. These two families have members that are symmetric to each other with respect to the $x - y$ plane (Jorba & Masdemont 1999). In our studies, the halo orbit we used is the one where most of the orbit is above the $x - y$ plane (the north halo). The halo orbit has two intersection points with the $x - z$ plane, and we choose the z coordinate of the upper intersection point as the out-of-plane amplitude parameter of the halo orbit. Figure 3 shows the curve of the stability parameter with respect to the amplitude parameter, with the left panel for the L_1 point and the right panel for the L_2 point. For the L_1 point, the continuation process is terminated at the point where $D < 0$ in Equation (12) (in this case, if $\alpha \neq 0$, the eigenvalues are complex with nonzero real parts). For the L_2 point, the continuation process is terminated when the out-of-plane amplitude reaches its maximum.

Judging from Figure 3, we know that with increasing amplitude, the stability parameter s_1 of the halo orbit reduces (Howell 1984). Since the motion around the halo orbit deviates from it at a speed proportional to $e^{at} \sim e^{s_1 t}$ (where a is the eigenvalue in Eq. (10)), the probe deviates at a slower speed for large halo orbits given the same initial deviation from the nominal orbit. Thus the control frequency could be smaller (Gómez et al. 1998a). From the view point of orbit control, it is better to use a larger halo orbit. Another reason for us to choose larger halo orbits is that they perform better in the OD process (see Sect. 4). Besides, larger halo orbits have better coverage on the Moon's surface and thus can improve the visibility between the CLP probes and lunar satellites (Hill et al. 2006).

2.3 DROs

The DRO family belongs to a special symmetric planar family of the CRTBP model which terminates onto a colliding orbit with the second primary (Szebehely 1967). For DROs that are very close to the Moon, the influence from the Earth is negligible, and the DROs are approximately retrograde circular orbits around the Moon in a two-body frame. This fact can be used to provide initial seeds for the numerical correction algorithm that calculates the periodic orbit. The left panel of Figure 4 shows several examples of DROs with different in-plane amplitudes. With increasing amplitudes, the Earth's influence becomes stronger and stronger and the shape of the DRO deviates further and further from a circular orbit. The right panel of Figure 4 shows the two stability parameters of this family before it collides with Earth. The abscissa of this panel is the x coordinate of the left intersection point of the orbit with the x axis. With increasing amplitudes, the planar stability parameter s_1 first comes down and then increases again. The same thing happens to the vertical stability parameter s_2. The ways to compute these stability parameters can be found in Hénon (1973). A brief outline is given here. There are three pairs of eigenvalues for the monodromy matrix of periodic orbits in the CRTBP model. For planar periodic orbits, the monodromy matrix has the following form

$$\boldsymbol{M} = \begin{pmatrix} m_{11} & m_{12} & 0 & m_{14} & m_{15} & 0 \\ m_{21} & m_{22} & 0 & m_{24} & m_{25} & 0 \\ 0 & 0 & m_{33} & 0 & 0 & m_{36} \\ m_{41} & m_{42} & 0 & m_{44} & m_{45} & 0 \\ m_{51} & m_{52} & 0 & m_{54} & m_{55} & 0 \\ 0 & 0 & m_{63} & 0 & 0 & m_{66} \end{pmatrix}. \tag{15}$$

The planar linearized motion around the planar periodic orbit is decoupled from the vertical linearized motion. The monodromy matrix can be decoupled into two matrices.

$$\boldsymbol{M_1} = \begin{pmatrix} m_{11} & m_{12} & m_{14} & m_{15} \\ m_{21} & m_{22} & m_{24} & m_{25} \\ m_{41} & m_{42} & m_{44} & m_{45} \\ m_{51} & m_{52} & m_{54} & m_{55} \end{pmatrix}, \qquad \boldsymbol{M_2} = \begin{pmatrix} m_{33} & m_{36} \\ m_{63} & m_{66} \end{pmatrix}. \tag{16}$$

For an autonomous Hamiltonian system such as the CRTBP, a trivial pair of eigenvalues is $(\lambda_1, \lambda_2) = (1, 1)$, so the planar stability parameter is defined as

$$s_1 = \lambda_3 + \lambda_4 = (m_{11} + m_{22} + m_{44} + m_{55}) - (\lambda_1 + \lambda_2) = (m_{11} + m_{22} + m_{44} + m_{55}) - 2 \tag{17}$$

and the vertical stability parameter is defined as

$$s_2 = \lambda_5 + \lambda_6 = (m_{33} + m_{66}). \tag{18}$$

From the stability criterion stated above and Figure 4, we know that these DROs are generally stable. Even in the real force model, they may become unstable, but they are still believed to have better stability properties than the CLP orbits (see the following Sect. 2.4). As a result, the frequency of orbit control maneuvers can be smaller.

Similar to the CLP case where the spatial halo family bifurcates from a vertical critical orbit in the planar Lyapunov family (Hou & Liu 2013), there is also a spatial periodic family bifurcating from the planar DRO family. The first step to find this spatial periodic family is to find the member with a vertical critical orbit in the planar DRO family. It is identified as the DRO orbit with a vertical stability parameter $s_2 = 2$ (the amplitude parameter is about $x = -0.27$ from the right panel of Fig. 4). The left panel of Figure 5 shows this critical DRO (denoted as “Planar” in the figure) and one member of the spatial family bifurcating from it (denoted as “3D” in the figure). The coordinate in Figure 5 is the barycentric synodic frame. To show the details, the positions of the Earth and Moon are not given in the pictures. The problem that arises from using these spatial periodic orbits is that they are too far away from the lunar satellite, and the long distance between the very large DROs and the lunar satellite is a disadvantage in the accuracy of the inter-satellite range data. As a result, the best choice is to choose some planar DROs with moderate amplitudes. To study the effects of the vertical components on the CAOD results, we only need to add a vertical displacement to the planar DROs. The resulting orbit is usually quasi-periodic in space, as shown in the right panel of Figure 5. This is the goal of our studies.

2.4 Real Force Model

The above studies about the two kinds of orbits are based on the CRTBP model. In the real force model of the Earth-Moon system, mainly two sources of perturbations exist: the Moon’s orbital eccentricity and the solar gravitational perturbation.

For the case of CLPs in the real force model, strictly speaking, the libration points lose their meaning as dynamical equilibrium points (Hou & Liu 2010, 2011), but the stability properties of the motions around these geometrical points does not change qualitatively. The motion is still exponentially unstable, and conditionally stable quasi-periodic orbits exist. These quasi-periodic orbits can be obtained via numerical approaches (Howell & Pernicka 1987; Gómez et al. 1998b). Figure 6 shows two quasi-halo orbits respectively around the L_1 (left) and L_2 (right) points in the real Earth-Moon system, lasting about two years and starting from the epoch J2000.0.

For the case of DROs, the case is a little more complicated. As mentioned above, the DROs are generated from the retrograde orbits circling the Moon. In the real force model, even with various perturbations, these orbits should still be stable for small amplitudes. The left panel of Figure 7 shows such a case. But with increasing amplitude, the DROs will become unstable and eventually escape from the Moon (Xu & Xu 2009), which is different from the case of the CRTBP model (see Fig. 4). The right panel of Figure 7 shows such a case. But even for this unstable case, the algorithm used to obtain quasi-periodic orbits in Figure 6 can still be used to find quasi-periodic DROs in the real force model. The details will not be reported here.

Generally, the stability properties of the DROs are better than the CLP orbits, even in the real force model (Xu & Xu 2009). This means a lower control frequency is needed to keep the probe around them. These better stability properties are the biggest advantage of DROs.

The way to generate Figure 7 is briefly stated as follows: Denote the initial state of the DRO in the CRTBP model as $\boldsymbol{r}_0$, $\dot{\boldsymbol{r}}_0$, and denote the transformation matrix from the instantaneous synodic frame to the inertial frame as C. We then have

$$\boldsymbol{R}_0 = kC\boldsymbol{r}_0, \qquad \dot{\boldsymbol{R}}_0 = \dot{k}C\boldsymbol{r}_0 + k\dot{C}\boldsymbol{r}_0 + kC\dot{\boldsymbol{r}}_0\,, \tag{19}$$

where $\boldsymbol{R}_0, \dot{\boldsymbol{R}}_0$ are the state vector in the inertial frame and k is the instantaneous distance between the Earth and the Moon. About the ways to compute the matrix C, readers can find details in Gomez et al. (2001).

3 ORBIT DETERMINATION ISSUES

3.1 OD Process

Denote the state vector of a lunar satellite or a probe as $\boldsymbol{X} \in \boldsymbol{R}^n$, then the equation of motion can be written in a compact form,

$$\dot{\boldsymbol{X}} = \boldsymbol{F}(\boldsymbol{X}, t). \tag{20}$$

Give an initial state $\boldsymbol{X}_0$ at the initial epoch t_0 and integrate Equation (20) to get an orbit. Denote the orbit as

$$\boldsymbol{X}(t) = \boldsymbol{\phi}(\boldsymbol{X}_0, t_0; t). \tag{21}$$

Usually, the observations $\boldsymbol{Y} \in \boldsymbol{R}^m$ are functions of the state vector and can be denoted as

$$\boldsymbol{Y} = \boldsymbol{Y}(\boldsymbol{X}, t) = \boldsymbol{Y}(\boldsymbol{X}_0, t_0; t). \tag{22}$$

Suppose we have a set of observations at the epochs $t_i (i = 1, \ldots, l)$. The goal of the OD process is to find $\boldsymbol{X}_0$ that satisfies

$$\boldsymbol{Y}(\boldsymbol{X}_0, t_0; t_1) = \boldsymbol{Y}_1, \ldots, \boldsymbol{Y}(\boldsymbol{X}_0, t_0; t_l) = \boldsymbol{Y}_l. \tag{23}$$

Usually $m \times l > n$. The Newton-Raphson method is taken to solve Equation (23) to obtain the least-squares solution. The iteration equations are

$$\Delta\boldsymbol{Y}_i = \frac{\partial \boldsymbol{Y}_i}{\partial \boldsymbol{X}_i}\frac{\partial \boldsymbol{X}_i}{\partial \boldsymbol{X}_0}\Delta\boldsymbol{X}_0 + \nu_i, \quad i = 1, \ldots, l, \tag{24}$$

where $\Delta\boldsymbol{Y}_i$ indicates the residuals of the observations, ν_i indicates the measurement noise and $\Delta\boldsymbol{X}_0$ are the corrections to the initial state vector $\boldsymbol{X}_0$.

There are many ways to process the measurement data (Tapley et al. 2004). In our work, the simple batch method is adopted. That means we generate the simulated data at one time and then perform the OD process using all the simulated data as one batch. A small trick is taken in the iteration process. The associated Euclidean norm is calculated as

$$\varepsilon = \sqrt{\sum_{i=1}^{N} |\Delta \boldsymbol{Y}_i|/N}. \tag{25}$$

At each iteration, we do not directly use $\Delta \boldsymbol{X}_0$ to correct the initial state vector $\boldsymbol{X}_0$, but use $\Delta \boldsymbol{X}_0/(1+\varepsilon)$. This trick can guarantee the convergence of the iteration process so that even a bad initial guess can return reliable values. We have to specially emphasize that different data processing approaches (such as the EKF method) may lead to results that are a little better than the ones in our work, but they will not change our conclusions qualitatively.

3.2 Data Generation

Usually, the CLP orbits (or the DROs) are described in the synodic frame, and the lunar orbit is described in the Moon-centered inertial frame. The OD process should be performed in a single frame. As a result, either we have to transform the state of the CLP orbits (or DROs) to the Moon-centered inertial frame, or we have to transform the state of the lunar satellite to the synodic frame. Considering the fact that it is more convenient to implement the perturbations in the real force model, we take the first approach. To generate the simulated data, we first transform the initial conditions of the CLP probe (or the DRO probe) to the Moon-centered inertial frame and integrate its orbit simultaneously with the lunar orbit. At each "observation" epoch, the inter-satellite range data are taken as the differences between their positions. In order to simplify our studies, only random errors (with a threshold) are considered to simulate the accuracy of the observation data. In our numerical simulations, three random error thresholds of 1, 10 and 100 m are considered. Generally, the OD accuracy is proportional to that of the observation data. To save space, only the results of the threshold of 1 meter are reported in our work. In the following simulations, without specifications, the sample interval is taken to be 10 minutes. One remark should be made. Different sample data with different intervals may lead to different OD results, but will not change the results qualitatively. Visibility analysis is not considered in the CRTBP model, but will be addressed in the real force model.

Two sub problems are considered. They are (1) CAOD of one CLP probe (or DRO probe) and one lunar satellite. In this case, the state vector contains 12 variables. They are the positions and velocities of the probe and the lunar satellite. This is the simplest case. (2) CAOD of two CLP probes (or DRO probes) and one lunar satellite. In this case, the state vector contains 18 variables. They are the positions and velocities of the two probes and the lunar satellite.

4 NUMERICAL SIMULATION I — THE CLP CASE

4.1 Sub Problem 1

The CAOD problem of a CLP probe and a lunar satellite is the most important and the most basic one in our studies. Here, the dependence of the OD accuracy on the length of data, the initial point, different CLP orbits and lunar orbits is given.

4.1.1 Length of data

We take a lunar orbit ($a = 1838\ \mathrm{km}, e = 0.0001, i = 90°, \Omega = \omega = M = 45°$) as an example. The out-of-plane amplitude of the halo orbit is taken to be $30\,780\ \mathrm{km}$ (for L_1 or L_2).

Table 1 The OD Results Corresponding to Different Lengths of Data (CLP)

Time (d)	Lunar Satellite			L_1 probe		Lunar Satellite			L_2 probe	
	R (m)	T (m)	N (m)	r (m)	$\dot{r}$ (m s^{-1})	R (m)	T (m)	N (m)	r (m)	$\dot{r}$ (m s^{-1})
1	0.15	147.41	90.37	3791.80	3.94×10^{-2}	0.28	156.49	121.70	2995.09	9.15×10^{-3}
2	0.11	1.31	3.51	118.60	8.50×10^{-4}	0.15	4.57	4.63	183.48	4.98×10^{-4}
5	0.10	0.29	0.26	10.97	5.60×10^{-5}	0.12	0.28	0.13	8.51	5.99×10^{-5}
10	0.05	0.11	0.06	0.24	1.26×10^{-6}	0.05	0.12	0.05	0.58	2.53×10^{-6}
15	0.03	0.06	0.06	0.16	7.81×10^{-7}	0.02	0.08	0.04	0.18	7.98×10^{-7}
20	0.02	0.05	0.05	0.10	5.06×10^{-7}	0.03	0.07	0.03	0.21	9.00×10^{-7}

Table 1 shows the results for the L_1 and L_2 points. In this table and all the following tables, the OD accuracy of the lunar satellite is expressed by the radial (R), transverse (T) and normal (N) errors, and that of the CLP probe is expressed by position error (r) and velocity error ($\dot{r}$). Our studies show that: (a) For the lunar satellite, the OD accuracy is unsatisfactory for 1-day length of data. However, it can be greatly improved for 2-day length of data; (b) For the CLP probe, the OD accuracy is unsatisfactory for a short length of data, but improves when the data length increases. This phenomenon can be explained like this. The period of the halo orbit around the two libration points is about 14 d. For a data length of a few days, the orbital arc of the CLP probe is too short to be determined accurately. For a longer time, the CLP probe can almost cover the overall halo orbit, so the OD accuracy increases; (c) For a short length of data, the OD accuracy of the lunar satellite is one or two magnitudes better than that of the CLP probe, but the difference improves for a long length of data.

In a word, it is enough to use a short length of data (several days) to recover the lunar orbit to the accuracy of the observation data, but it requires a longer length of data ($\sim$ 10 d) for the CLP probe. For some other numerical simulations done by us, the same conclusions hold.

4.1.2 Initial point on the halo orbit

In the following, the point from which we start the observation will be called the initial point. It is also the point for which we estimate its state vector in the OD process. Table 1 corresponds to the case where we choose the point on the halo orbit with the maximum z coordinate as the initial point for the CLP probe. However, the geometry between the lunar satellite and the CLP probe is constantly changing in a fixed arc. Different initial points are chosen, so different OD results can be expected. Figure 8 gives an illustrative picture of different initial points on a halo orbit. τ is the period of the halo orbit.

In our numerical simulations, one hundred initial points are taken. Figure 9 shows the 2-day (left panel) and 15-day (right panel) OD results for the L_1 probe and lunar satellite. From Figure 9, we draw the following conclusions: for a short length of data, the OD accuracy vibrates wildly with respect to the initial point and the vibration width is large; for a longer length of data, the vibration becomes smoother and the vibration width also reduces. The reason for this difference lies in the fact that a short length of data can only cover a small portion of a halo orbit and the OD accuracy is sensitive to different initial points, but a long length of data can cover nearly the whole halo orbit and thus makes the OD accuracy less sensitive to different initial points.

4.1.3 Amplitude of halo orbit

Here, we study the effects of the amplitude of the halo orbit on the CAOD results. To reduce the effects of different initial points discussed above, the length of data is taken to be 15 d.

Figure 10 shows the relation curve between the OD accuracy and the out-of-plane amplitude of the halo orbit around the L_1 point. The left panel shows the results when the point $\tau_0 = 0$ is used as the OD initial point, and the right panel shows the results when the point $\tau_0 = \frac{1}{2}\tau$ is used as the OD initial point. Obviously, the OD accuracy of the lunar satellite is generally on the level of the observation data ($\leq 1m$) for both panels. However, the OD accuracy for the CLP probe shows an obvious tendency to reduce (from several meters to be less than 1 meter) with increasing amplitudes in both panels. The obvious decreasing tendency for the CLP probe in Figure 10 delivers the following important information to us: the OD accuracy of the CLP probe is better for larger halo orbits. Although only the results corresponding to $\tau_0 = 0$ and $\tau_0 = \frac{1}{2}\tau$ are given, our numerical simulations for other different initial points show no qualitative difference.

4.1.4 Orbital elements of lunar satellites

Now we study the effects of the orbital elements of lunar satellites. Similar to 4.1.3, the length of data is taken to be 15 d. The initial point on the halo orbit is chosen as $\tau_0 = 0$. The out-of-plane amplitude of the halo orbit is $30\,780$ km. Figure 11 gives these OD results corresponding to different orbital elements of the lunar satellite. Generally, the effects of the lunar orbits on the OD accuracy are much milder than those of the halo orbits. L_2 has similar results as L_1.

4.1.5 Conclusions

From the results of sub problem 1 in 4.1.1–4.1.4, we summarize our conclusions as follows: (a) for lunar satellites, a short length of data is enough to recover the orbit to the level of observations, but for the CLP probe, this accuracy usually requires a data length of about 10 d or ever longer; (b) for a short length of data, different initial points of the halo orbit influence the OD accuracy, but this influence becomes weaker for a longer time; (c) different orbital elements of the lunar satellite have little effect on the OD accuracy; (d) halo orbits with large out-of-plane amplitudes are preferred for three reasons: better stability properties, better lunar surface coverage (and visibility from the lunar satellites) and better OD accuracy.

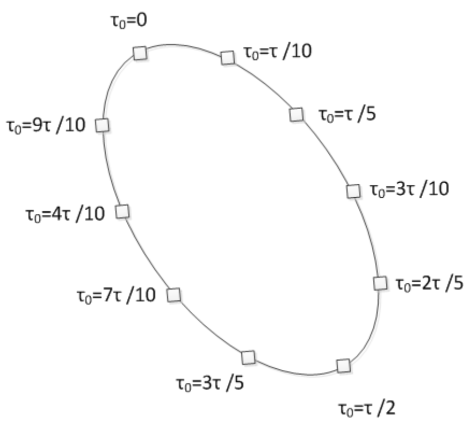

Fig. 8 An illustrative picture describing different points on a halo orbit used as the initial point of the OD process.

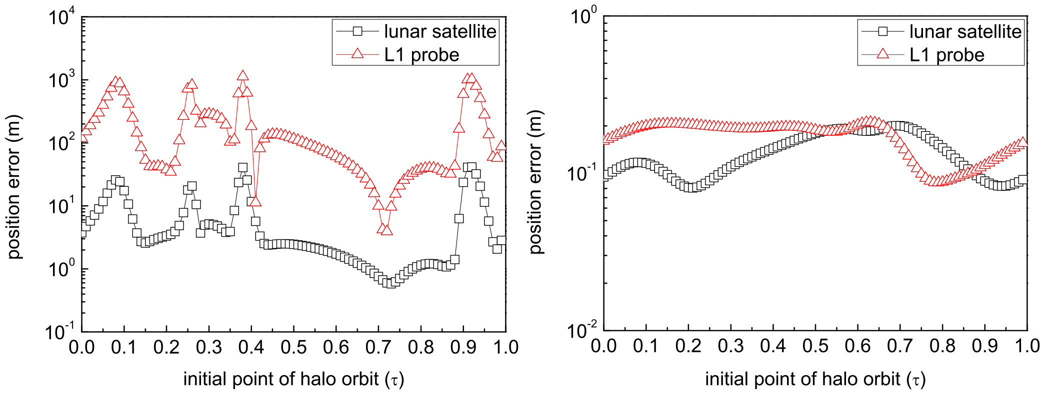

Fig. 9 The OD results corresponding to different initial points of a halo orbit around L_1. *Left*: 2-day length of data; *Right*: 15-day length of data. The out-of-plane amplitude of the halo orbit is chosen as $30\,780$ km.

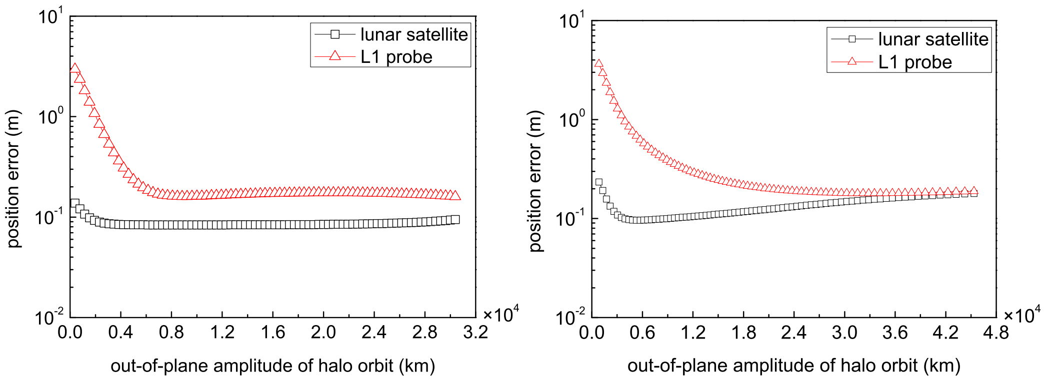

Fig. 10 The relation between the OD accuracy and the out-of-plane amplitude of the halo orbit around the point L_1. The length of data is 15 d. *Left:* $\tau_0 = 0$. *Right:* $\tau_0 = \frac{1}{2}\tau$.

4.2 Sub Problem 2

In this subsection, we consider the CAOD problem of two CLP probes and one lunar satellite. The addition of the second CLP probe adds two extra inter-satellite data: the range data between the lunar satellite and the new CLP probe, and the range data between the two CLP probes. The purpose of this research is to study whether there are any improvements in the CAOD results with the addition of another CLP probe.

There are many possibilities in this sub problem. For example, the two probes can be around the same CLP (L_1 or L_2), on the same halo orbit or on two different halo orbits. The two probes can also be around different CLPs, on halo orbits with large or small amplitudes. A detailed statement of the numerical results is lengthy and unnecessary. Here, we only give the general conclusions: (1) Compared with sub problem 1, no obvious improvement has been observed for a long length of data; (2) The OD accuracy for a short length of data does show some improvement compared with sub problem 1.

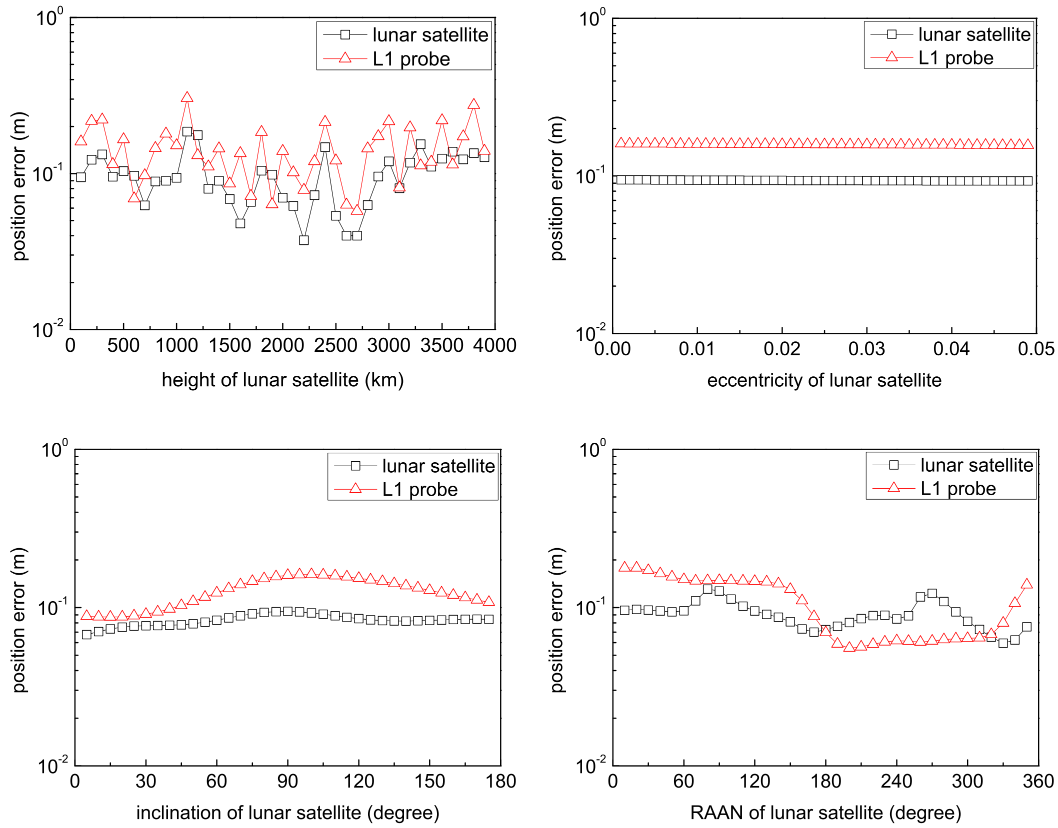

Fig. 11 15-day OD results corresponding to different orbital elements of a lunar satellite. *Upper left*: $e = 0.0001$, $i = 90°$, $\Omega = \omega = M = 45°$; *Upper right*: height = 100 km, $i = 90°$, $\Omega = \omega = M = 45°$; *Bottom left*: height=100 km, $e = 0.0001$, $\Omega = \omega = M = 45°$; *Bottom right*: height = 100 km, $e = 0.0001$, $i = 90°$, $\omega = M = 45°$.

Figure 12 shows the contour maps of the position error (unit m) with respect to different initial points on two halo orbits (one is around L_1 and the other is around L_2), for data length of 2 d. The L_1 halo orbit is the same as the one in Figure 9, and the out-of-plane amplitude of the L_2 halo orbit is 15 365 km.

From the left panel of Figure 9, we notice that there are some abrupt changes in the OD accuracy for the L_1 probe. We think these abrupt changes are due to the poor geometry between a lunar satellite and a CLP probe for a short length of data. The addition of the second CLP probe helps improve the geometry (by adding more constraints, i.e. observation data). The direct result is that the irregularity in Figure 9 (the OD accuracy in Fig. 9 can vibrate from several meters to about 1 km for different points) has been reduced (the maximum value of the OD accuracy in Fig. 12 is less than 200 m).

Several remarks should be made:

Remark 1: The CAOD process for a short length of data is necessary. The CLP orbits are generally highly unstable. A small deviation without control may grow exponentially (Hou et al. 2011). In theoretical studies, we can determine the CLP orbit accurately using a simulated long length of data. But in practice, due to the unavoidable errors, usually a station-keeping maneuver is performed every several days. In such a case, it is necessary to determine the orbit of the CLP probe within a short length of data.

Remark 2: Although the case of two L_1 probes (or two L_2 probes) can also enhance the performance of the system, the configuration of one L_1 probe and one L_2 probe is recommended. The reason is that in this case a better lunar surface coverage can be achieved. Besides, a better visibility between the CLP probes and the lunar satellite can also be achieved: when the lunar satellite is invisible to one CLP probe, it is usually visible to the other one.

Remark 3: In Figure 12, we give the OD results corresponding to one large L_1 halo orbit and one small L_2 halo orbit. We find the system performs better than the case of two large halo orbits (although the improvement is mild). The reason can be qualitatively explained like this: the lunar satellite is dominated by the Moon's central gravitational force but the two CLP probes are simultaneously dominated by the Earth and the Moon. Qualitatively speaking, a halo orbit with a larger out-of-plane amplitude is more affected by the Earth than a halo orbit with a smaller out-of-plane amplitude. Thus, the difference in force environments of the three orbiters (one lunar satellite plus two CLP probes) is more obvious in this case than in the case of two large halo orbits. Therefore, our recommendation is to use halo orbits with different in amplitudes for the two CLP probes.

5 NUMERICAL SIMULATION II—THE DRO CASE

This section studies the CAOD problem of a lunar satellite and the DRO probes. The results are compared with those of the CLP probes. Some conclusions are the same as those of the CLP case: the lunar satellites have little effect on the CAOD results; the OD accuracy improves with a longer data length; the OD accuracy depends on different initial points for the DRO, but this difference becomes smaller and smoother with a longer data length. The performance of the system for a short length of data can be improved by adding another DRO probe to the system. However, there are also some differences. To save space, we only report the aspects that are different.

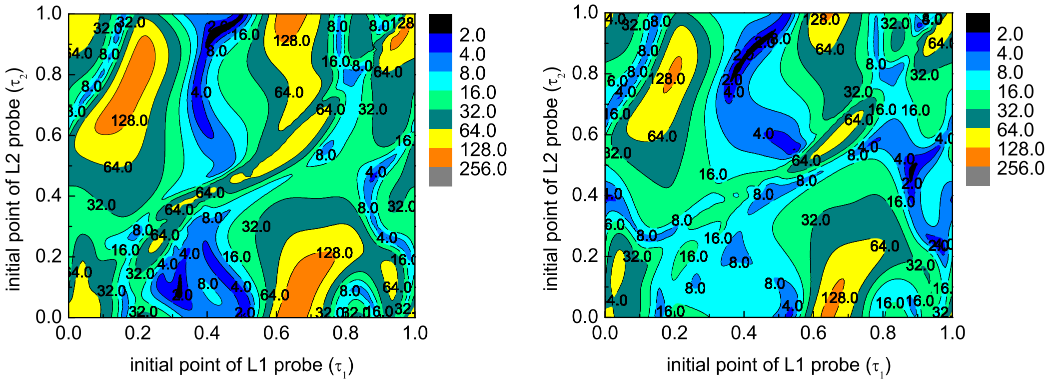

Fig. 12 Contour maps of the position error with respect to different initial points on a large halo orbit around the L_1 point and a small halo orbit around the L_2 point. *Left*: position error of L_1 probe; *Right*: position error of L_2 probe. The length of data is 2 d. The out-of-plane amplitude of the halo orbit around L_1 is 30 780 km, and the out-of-plane amplitude of the halo orbit around L_2 is 15 365 km.

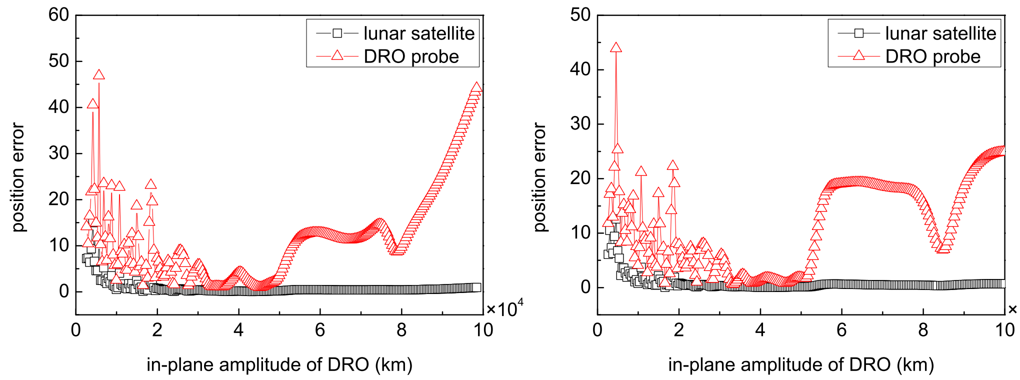

Fig. 13 The relation between the OD accuracy and the in-plane amplitude of the DROs. *Left*: $T_0 = 0$; *Right*: $T_0 = \frac{1}{2}T$.

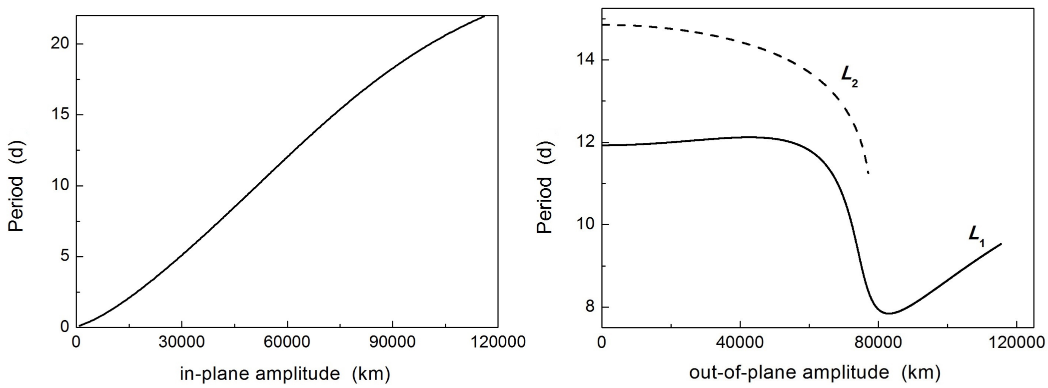

Fig. 14 The relation between the orbital period and the amplitude parameter. *Left*: the relation between the orbital period and the in-plane amplitude of the DRO; *Right*: the relation between the orbital period and the out-of-plane amplitude of the halo orbit.

5.1 In-plane Amplitude

The DRO family is a planar family in the CRTBP model. As a result, the in-plane amplitude is chosen as the amplitude parameter of this family. This section studies how the OD accuracy changes with the in-plane amplitude.

Figure 13 shows the relation curves of the OD accuracy with respect to the in-plane amplitude of the DRO orbits. The left panel is for initial point $T_0 = 0$ and the right panel is for initial point $T_0 = \frac{1}{2}T$. T is the period of the DRO. The length of the data is 15 d. The lunar orbit has parameters $(a = 1838\ \mathrm{km}, e = 0.0001, i = 90°, \Omega = \omega = M = 45°)$.

Different from the CLP case, the OD accuracy is not better when the in-plane amplitude grows larger. The best performance corresponds to the amplitude around 4.5×10^4 km. The reason can be qualitatively explained as this: the period of the DRO orbit grows significantly with increasing amplitude, as shown in the left panel of Figure 14. Fix the length of data (for example, 15 d). For a smaller DRO, it can travel several loops, but the influence from the Earth is mild, so the OD accuracy

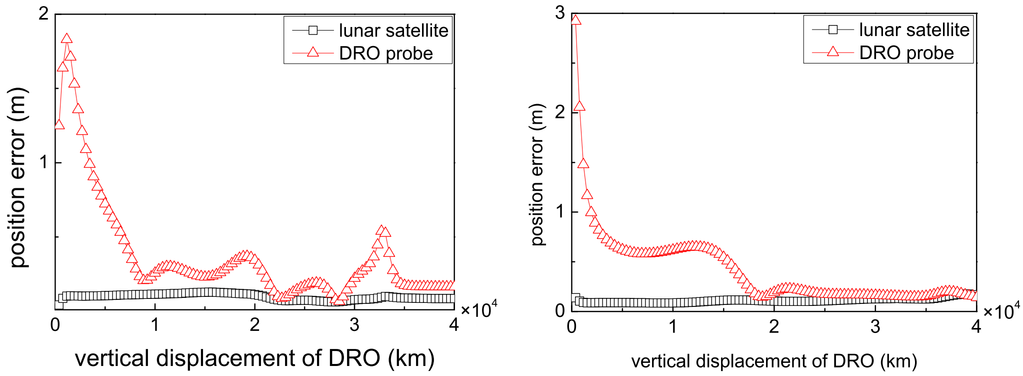

Fig. 15 The relation between the OD accuracy and the vertical displacement of DROs. *Left*: $T_0 = 0$; *Right*: $T_0 = \frac{1}{2}T$.

Table 2 The OD Results Corresponding to Different Lengths of Data (DRO)

Time (d)	Lunar Satellite			DRO probe	
	R (m)	T (m)	N (m)	r (m)	$\dot{r}$ (m s^{-1})
1	0.30	599.47	460.75	9130.95	1.60×10^{-1}
2	0.15	8.71	37.96	1178.17	5.22×10^{-3}
5	0.10	0.85	6.01	147.89	1.20×10^{-3}
10	0.01	0.17	0.34	8.90	6.87×10^{-5}
15	0.01	0.07	0.14	4.13	3.29×10^{-5}
20	0.01	0.16	0.24	6.58	5.10×10^{-5}

is not good. For a very large DRO, the influence from the Earth is strong, but it cannot even cover a single loop due to the long period, so the OD accuracy is not good either. The best OD results should have medium sizes. This phenomenon does not happen for halo orbits. The right panel of Figure 14 shows the orbital period versus out-of-plane amplitude of the halo family. The dashed line is for L_2 and the solid line is for L_1. With increasing amplitude, the period of the halo family around L_2 reduces. The period of the halo family around L_1 does not reduce monotonically, but it is generally smaller for larger halo orbits. Table 2 shows the OD results for a DRO orbit with the in-plane amplitude $40\,713$ km. It seems that the OD accuracy is not as good as that of the CLP case (for example, a 15-day length of data can only produce a position error of 4.13 m for the DRO probe and 0.17 m for the lunar satellite). In the following section, we will see how to improve the OD results by adding vertical displacement to the DRO orbit.

5.2 Vertical Displacement

In this subsection, we study the effects of the vertical displacement on the DROs. As we mentioned in Section 2.3, to fulfill this study, we can simply add a vertical displacement to the DRO for different initial points. Using the same DRO as Table 2, Figure 15 shows the curve of the OD accuracy with respect to the increasing vertical displacement. The left panel shows the results when the vertical displacements are added to the leftmost point of the DRO, and the right panel shows the results when the vertical displacements are added to the rightmost point of the DRO. It seems that for the DRO probe, the OD results are better with larger vertical displacements (although the improvement is not very obvious).

Table 3 shows one example. The vertical displacement is $19\,237$ km. The reason for this improvement, in our opinion, is a better relative geometry between the DRO probe and the lunar satellite in space: viewing in the Earth-centered inertial frame, the orbit of the lunar satellite is restricted to be in a region very close to the Moon's orbital plane. The DRO is also restricted to be within the Moon's orbital plane. The relative geometry between the two is bad because they are in the same plane (the Moon's orbital plane). By adding a vertical displacement to the DRO, the relative geometry can be improved. Actually, we think the same reason can also explain why halo orbits with larger out-of-plane amplitudes perform better in the CLP case (see Sect. 4.1.3).

Table 3 The OD Results Corresponding to Different Lengths of Data (DRO with the vertical displacement)

Time (d)	Lunar Satellite			DRO probe	
	R (m)	T (m)	N (m)	r (m)	$\dot{r}$ (m s^{-1})
1	0.28	1.34	7.13	232.79	1.29×10^{-3}
2	0.25	3.78	3.30	116.31	9.31×10^{-4}
5	0.08	0.17	0.16	6.48	3.89×10^{-5}
10	0.05	0.16	0.05	0.34	1.96×10^{-6}
15	0.03	0.10	0.05	0.37	2.07×10^{-6}
20	0.02	0.06	0.05	0.30	1.84×10^{-6}

6 REAL FORCE MODEL

6.1 Force Model Description

Different from the CRTBP model, the orbits of the CLP probe (or DRO probe) and the lunar satellites are integrated in the selenocentric mean equatorial frame at the epoch J2000.0. For the lunar satellite, the perturbations considered are a non-spherical gravitational perturbation of the Moon and a point mass gravitational perturbation from the Earth and the Sun. For the CLP orbit (or the DRO), although the non-spherical terms of the Moon's gravity field are negligible, they are also considered because the CAOD process is fulfilled in the same force model.

In the following numerical simulations: the lunar gravity field model is taken to be LP75G (degree and order is chosen up to 10° and 10 respectively); the positions of the Earth and Sun are given by the numerical ephemeris DE405; the initial epoch is starting from 58849.0MJD.

6.2 Visibility Analysis

In practical observations, the lunar satellite and spatial probe are not always visible to each other. When the lunar satellite is on the far side of the Moon and invisible to the probe, the observations cannot be obtained.

Figure 16 is an illustrative picture of the visibility between the lunar satellite and the probe. The invisible region satisfies the condition

$$\angle \mathrm{OHL} < \angle \mathrm{OHA} \quad \text{and} \quad \mathrm{HL} > \mathrm{HA}\,,$$

where A is the point of tangency and R is the equatorial radius of the Moon.

6.3 One Numerical Example

As an example, we only give the simplest case of a CLP probe (or DRO probe) and a lunar satellite. The purpose of this study is to demonstrate the feasibility of the CAOD process in the real force

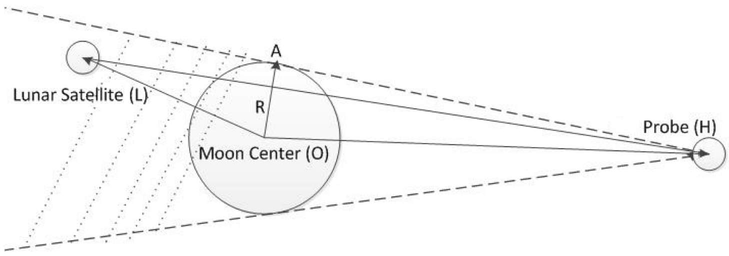

Fig. 16 The visibility between the lunar satellite and the probe.

Table 4 The OD Results Corresponding to Different Lengths of Data in the Real Force Model and the CRTBP Model of the Earth-Moon System

Time (d)	Lunar Satellite						L_1 probe			
	R^c (m)	R^a (m)	T^c (m)	T^a (m)	N^c (m)	N^a (m)	r^c (m)	r^a (m)	$\dot{r}^c$ (m s^{-1})	$\dot{r}^a$ (m s^{-1})
1	0.27	0.15	112.21	147.41	45.58	90.37	2290.45	3791.80	1.33×10^{-2}	3.94×10^{-2}
2	0.20	0.11	11.40	1.31	7.00	3.51	291.53	118.60	2.90×10^{-3}	8.50×10^{-4}
5	0.09	0.10	0.46	0.29	0.36	0.26	22.52	10.97	1.49×10^{-4}	5.60×10^{-5}
10	0.07	0.05	0.13	0.11	0.10	0.06	1.19	0.24	7.51×10^{-6}	1.26×10^{-6}
15	0.06	0.03	0.13	0.06	0.06	0.06	0.72	0.16	5.08×10^{-6}	7.81×10^{-7}
20	0.05	0.02	0.19	0.05	0.05	0.05	0.52	0.10	3.57×10^{-6}	5.06×10^{-7}

Time (d)	Lunar Satellite						DRO probe			
	R^c (m)	R^b (m)	T^c (m)	T^b (m)	N^c (m)	N^b (m)	r^c (m)	r^b (m)	$\dot{r}^c$ (m s^{-1})	$\dot{r}^b$ (m s^{-1})
1	0.36	0.28	75.61	1.34	26.71	7.13	688.73	232.79	1.65×10^{-2}	1.29×10^{-3}
2	0.12	0.25	8.73	3.78	6.37	3.30	203.74	116.31	2.20×10^{-3}	9.31×10^{-4}
5	0.06	0.08	0.18	0.17	0.17	0.16	6.79	6.48	3.69×10^{-5}	3.89×10^{-5}
10	0.04	0.05	0.11	0.16	0.08	0.05	1.21	0.34	6.96×10^{-6}	1.96×10^{-6}
15	0.02	0.03	0.06	0.10	0.07	0.05	0.49	0.37	2.70×10^{-6}	2.07×10^{-6}
20	0.01	0.02	0.04	0.06	0.05	0.05	0.19	0.30	1.03×10^{-6}	1.84×10^{-6}

Notes: ^{a} The OD results for the CRTBP model in Table 1; ^{b} The OD results for the CRTBP model in Table 3; ^{c} The OD results for the real force model.

model. The same initial conditions of the lunar satellite and the probe as Table 1 and Table 3 are used, but they are integrated in the real force model this time. Table 4 shows the OD results in the real force model and the CRTBP model of the Earth-Moon system. From Table 4, we know that the results in the real force model are similar to those of the CRTBP model. Although we did not do other numerical tests, we believe that all the conclusions in the CRTBP model can be simply extended to the real force model.

7 DISCUSSION

Discussion 1: Although all the studies above are based on inter-satellite range data, it is also possible to use other types of inter-satellite data, such as the azimuth and elevation angles of the CLP probe (or DRO probe) with respect to the lunar satellite. We did some numerical simulations with this type of observation data. Our results show that the OD accuracy can also reach that of the observation data. To save space, no details will be presented here.

Discussion 2: In all of our numerical simulations (even in the case of the real force model), we did not consider the orbit maneuvers. In practice, due to the instability of the CLP orbits (or DROs),

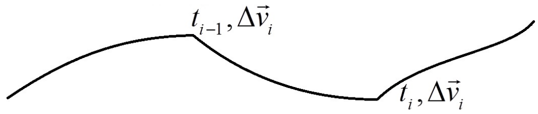

Fig. 17 An illustration of the orbit maneuvers for station-keeping of the CLP probe.

orbit maneuvers are necessary and the OD process covering a long length of data should take these maneuvers into consideration.

In the case of the CLP probe, the CAOD process with only a short length of data is usually necessary. The strong instability of the CLP probe needs highly frequent orbital control and each maneuver requires precise information about the CLP orbit. This means we have to determine the CLP orbit between two consecutive maneuvers, as illustrated in Figure 17. Suppose a maneuver $\Delta \boldsymbol{v}_{i-1}$ at epoch t_{i-1} is already done and another maneuver $\Delta \boldsymbol{v}_i$ is scheduled in the coming epoch t_i. If we know precise information about the previous maneuver $\Delta \boldsymbol{v}_{i-1}$, we can use a longer orbital data length (the orbital data previous to t_{i-1} and the orbital data between t_{i-1} and t_i) to determine the state at epoch t_i. However, sometimes we do not know enough information about the previous maneuver $\Delta \boldsymbol{v}_{i-1}$ (in the case of a maneuver malfunction or in the case of the first maneuver $i = 1$). In this case, we have to determine the orbit by only using the orbit between t_{i-1} and t_i) (which is usually short). Postponing the coming maneuver (i.e., increasing the length between t_{i-1} and t_i) can enhance the OD accuracy, but it may also increase the burden imposed by the maneuver (in the worst case, it may cause a failure of the mission) because the probe may deviate further if the coming maneuver $\Delta \boldsymbol{v}_i$ is performed too late.

In the case of the DRO probe, the situation is better. As we have stated in Sections 2.3 and 2.4, the DRO orbits usually have better stability properties than the CLP orbit. This better stability allows us to increase the length of an orbit between two consecutive maneuvers so that we can determine the orbit more accurately. Even though the probe may deviate a little further due to the late maneuver, it will not deviate too far due to the mild instability.

Discussion 3: The reason for the feasibility of the CAOD process in this paper is that the introduction of the special probes (the CLP probes or the DRO probes) introduces the Earth's gravitational force into the system, which significantly breaks the rotational symmetry of the gravitational field with respect to Moon's center. However, an obvious disadvantage of the CAOD process in this paper is the low accuracy of the OD results for the special probes with a short length of data. This is inherently related to the long period of these special orbits. If a special orbit with a period comparable to that of the lunar satellite but in a force environment significantly different from the Moon's gravitational force is introduced into the system, this problem will be greatly improved. One way to achieve this goal is to introduce a lunar satellite with a very large solar sail. We are currently working on this issue.

8 CONCLUSIONS

In this paper, the CAOD problem between a lunar satellite and a probe on some special orbits are studied. Two kinds of special orbits are investigated: the CLP orbits and the DROs. From our studies, the following conclusions can be made.

(1) The CAOD process is theoretically feasible. It requires several days to determine the orbit of the lunar satellite with respect to the accuracy of the observations over several days, but it requires a longer time ($\sim$10 d) for the CLP orbit or the DRO to achieve the same accuracy;

(2) For the CLP case, halo orbits with larger out-of-plane amplitudes are recommended. They have better stability properties, better visibility between the Moon and the lunar satellite and better performance in the CAOD process;
(3) For the DRO case, medium sized DROs ($\sim$45 000 km) perform best in the CAOD process. The relative geometry between the lunar satellite and the DRO probe can be improved by adding vertical displacement to the DROs, which affects the CAOD results;
(4) Sometimes, the CAOD process must be done with a short length of data. In this case, adding another or more CLP probes or DRO probes may improve the observation geometry of the system, and thus can enhance the performance of the system;
(5) Only judging from the stability of the special orbits, DROs are preferred. Although large DROs may also become unstable in the real force model, their instability should be milder than that of the CLP orbits. As a result, a lower control frequency of maneuvering in the orbit is possible. Due to the lower control frequency, a longer length of data between two consecutive orbit maneuvers is also possible, which is favorable for the CAOD process.

Acknowledgements This work has been supported by the National Natural Science Foundation of China (Grant Nos. 11033009, 11078001 and 11203015), the National Basic Research Program of China (973 Program, Grant No. 2013CB834100) and the National High-tech R&D Program of China (863 Program, Grant No. 2012AA121602).

References

Arnol'd, V. I. 1999, Mathematical Methods of Classical Mechanics (2nd ed., Beijing: World Publishing Corporation)
Bell, D. J., Cesarone, R., Ely, T., et al. 2000, in Aerospace Conference Proceedings, 2000 IEEE, 7, 75
Bray, T. A., & Goudas, C. L. 1967, Advances in Astronomy and Astrophysics, 5, 71
Carpenter, J. R., Folta, D. C., Moreau, M. C., et al. 2004, in AIAA/AAS Astrodynamical Specialist Conference, 4747
Chung, M. J., Hatch, S. J., Kangas, J. A., et al. 2010, in AIAA/AAS Astrodynamical Specialist Conference, 8384
Doedel, E. J. 1981, Congressus Numerantium, 30, 265
Doedel, E. J., Romanov, V. A., Paffenroth, R. C., et al. 2007, International Journal of Bifurcation and Chaos, 17, 2625
Farquhar, R. W. 1967, Journal of Spacecraft and Rockets, 4, 1383
Farquhar, R. W. 1972, Astronaut Aeronaut, 10, 59
Farquhar, R. W., Dunham, D. W., Guo, Y., & McAdams, J. V. 2004, Acta Astronautica, 55, 687
Folta, D. C., Woodard, M., Howell, K., Patterson, C., & Schlei, W. 2012, Acta Astronautica, 73, 237
Gómez, G., Howell, K. C., & Masdemont, J. 1998a, Adv Astronaut Sci., 99, 949
Gómez, G., Masdemont, J., & Simó, C. 1998b, Journal of the Astronautical Sciences, 46, 135
Gómez, G., Llibre, J., Martınez, R., & Simó, C. 2001, Dynamics and Mission Design Near Libration Point Orbits–Volume 1: Fundamentals: The Case of Collinear Libration Points (Singapore: World Scientific)
Hénon, M. 1973, Celestial Mechanics, 8, 269
Hill, K., & Born, G. 2007, Journal of Guidance Control Dynamics, 30, 679
Hill, K., Born, G. H., & Lo, M. W. 2005a, in AAS/AIAA Astrodynamics Specialist Conference, 400
Hill K., Lo M. W., Born G. H., 2005b, in AAS/AIAA Astrodynamics Specialist Conference, 399
Hill, K., Parker, J. S., Born, G. H., et al. 2006, in AIAA/AAS Astrodynamics Specialist Conference and Exhibit, 6662
Hirabayashi, H., Hirosawa, H., Kobayashi, H., et al. 2000, PASJ, 52, 955
Hoffman, T. L. 2009, in Aerospace conference, 2009 IEEE (doi: 10.1109/AERO.2009.4839327)

Hou, X. Y., & Liu, L. 2010, Celestial Mechanics and Dynamical Astronomy, 108, 301
Hou, X. Y., & Liu, L. 2011, Celestial Mechanics and Dynamical Astronomy, 110, 71
Hou, X., Liu, L., & Tang, J. 2011, Advances in Space Research, 47, 1127
Hou, X. Y., & Liu, L. 2013, Celestial Mechanics and Dynamical Astronomy, 116, 241
Howell, K. C. 1984, Celestial Mechanics, 32, 53
Howell, K. C., & Pernicka, H. J. 1987, Celestial Mechanics, 41, 107
Jorba, À., & Masdemont, J. 1999, Physica D Nonlinear Phenomena, 132, 189
Kato, M., Sasaki, S., Tanaka, K., Iijima, Y., & Takizawa, Y. 2008, Advances in Space Research, 42, 294
Li, Y. H., Zheng, J., Yi, K. C., 2007, Chin J Space Sci, 27, 227
Liu, L., & Liu, Y. C. 2000, J spacacraft TT&C Technol, 19, 13 (in Chinese)
Liu, Y. C., Liu, L., & Wang, C. B. 2000, J spacacaft TT&C Technol, 19, 7 (in Chinese)
Liu, Y. C., Zhang, F. P., Dong, X. J. 2003, J Spacecraft TT&C Technol, 22, 54 (in Chinese)
Muñoz-Almaraz, F. J., Freire, E., Galán, J., et al. 2003, Physica D Nonlinear Phenomena, 181, 1
Richardson, D. L. 1980, Celestial Mechanics, 22, 241
Sheikh, S. I., Pines, D. J., Ray, P. S., et al. 2006, Journal of Guidance Control Dynamics, 29, 49
Szebehely, V. 1967, Theory of Orbits. The Restricted Problem of Three Bodies (New York: Academic Press)
Tapley, B. D., Schutz, B. E., Born, G. H., et al. 2004, Statistical Orbit Determination, 200 (Burlington: Elsevier Academic Press)
Wang, D. Y., & Huang, X. Y. 2009, Aerosp Control Appl, 35, 6 (in Chinese)
Xu, M., & Xu, S. 2009, Acta Astronautica, 65, 853 (in Chinese)
Yim, J. R., Crassidis, J. L., & Junkins, J. L. 2004, in AAS/AIAA Astrodynamics Specialist Conference, 257